Flexural behaviour of a novel bamboo-plywood sandwich composite panel

Author

Darzi, S, Karampour, H, Gilbert, BP, Bailleres, H

Published

2018

Conference Title

WCTE 2018 - World Conference on Timber Engineering

Version

Version of Record (VoR)

WCTE 2018
2018 World Conference on Timber Engineering
August 20 - 23, 2018 | Seoul, Republic of Korea

FLEXURAL BEHAVIOUR OF A NOVEL BAMBOO-PLYWOOD SANDWICH COMPOSITE PANEL

Siavash Darzi[1], Hassan Karampour[2], Benoit P.Gilbert[3], Henri Bailleres[4]

ABSTRACT: Numerical investigation of the flexural behaviour of an innovative sandwich composite panel is presented. The panel consists of outer structural plywood skins and an inner core of vertically aligned hollow bamboo rings and is referred to as Bamboo Core Sandwich (BCS). The flexural behaviour of the BCS panel under one-way and two-way bending is investigated using the Ritz-method. The Ritz-model is validated against published results of an experimental test conducted on GFRP sandwich panels. The effects of the thickness of the plywood skins and height of the bamboo core on the bending stiffness of BCS panels are presented. The results are compared to the bending stiffness of Cross-laminated Timber (CLT) panels of almost similar depths. Results indicate that at almost identical bending stiffness, the proposed sandwich composite panel can be thinner and substantially lighter than existing commercial CLT panels.

KEYWORDS: Sandwich panel, Bamboo core, Ritz method, Cross-laminated Timber (CLT)

1 INTRODUCTION

In structural engineering applications, sandwich elements are typically fabricated by attaching two thin and stiff skins, to a lightweight, flexible and relatively thick core. Sandwich panels are extensively used in automotive, aerospace, marine and industrial applications due to their high strength-to-weight and stiffness-to-weight ratios. Recently, there has been a growing trend in the construction industry to use sandwich structural elements such as floors and load bearing walls [1]. Common skin materials include thin metal sheets [2], fibre reinforced polymer (FRP) composites [3] and in some structural applications, reinforced concrete [4]. Core materials include balsa wood [5], polymeric foams [6], FRP reinforced foam cores [7] metallic foams [8,9] and honeycomb cells [10]. With recent changes in legislations and the growing trend towards tall mass-timber buildings, engineered wood products such as Cross-laminated Timber (CLT) have gained increased popularity in residential and non-residential construction in form of roof, floor and wall applications. CLT is defined as a prefabricated solid engineered wood product made of an odd number of orthogonally bonded layers of solid sawn lumbers using adhesive, nails or wooden dowels [11]. A CLT panel configuration is shown in Figure 1(a). Although CLT is a lighter alternative compared to composite and concrete slabs/walls, properly designed timber sandwich panels may be more efficient. A major area where sandwich panels are beneficial is in flooring systems. Due to their lightweight and strength properties, the use of sandwich panels may prove better alternative, which results in reduced overall load and hence the advantage of using smaller supporting members.

Although there exists a wide range of composite sandwich panels, most of the currently used core materials are not appropriate for structural applications. Normally, the core material is made of low strength foam material. Research has shown that the behaviour of sandwich panels is strongly affected by the nature of the core material [12]. The role of the core is critical in transmitting the shear between the face in compression and the one in tension. It has been observed that most sandwich elements fail due to delamination of the skins from the core or shear failure of the core [13]. Therefore, it is necessary to fully understand the shear behaviour of the core and behaviour of the panel as a whole to maximize the performance of the sandwich construction and fully utilise its load bearing capacity.

Several researchers have used high-density core material to improve the shear carrying capacity of the sandwich structures. Accordingly, Daniel and Abot [14] filled the cells of the honeycomb core with epoxy to prevent premature shear failure of the composite sandwich at the load application. In another study on short beams, Dai and Thomas Hahn [15] measured higher shear strength for H-250 PVC foam core than for D-100 balsa wood core. However, such advantage disappeared as the floor span becomes longer. Mahfuz et al. [16] improved the performance of composite sandwich under flexure by infusing titanium dioxide (TiO2) nanoparticles into the parent polyethylene foam material to strengthen the core structure. Their results showed that a 53% increase in the

[1] Siavash Darzi, Griffith University, Gold Coast, Australia, siavash.darzi@griffithuni.edu.au
[2] Hassan Karampour, Griffith University, Gold Coast, Australia, h.karampour@griffith.edu.au
[3] Benoit P. Gilbert, Griffith University, Gold Coast, Australia, b.gilbert@griffith.edu.au
[4] Henri Bailleres, Department of Agriculture and Fisheries, Brisbane, Australia, Henri.Bailleres@daf.qld.gov.au

flexural strength could be attained by infusing 3% loading of TiO2 nanoparticles in the core.

The previously mentioned studies showed that the enhancement of the core material significantly improves the performance of the composite sandwich structures. The drawback however, is that the weight and the production cost of these composite sandwiches are also significantly increased. To address these drawbacks, a new type of lightweight sandwich panel with vertically aligned hollow bamboo rings and commercial plywood sheets (skins) is proposed here. The hollow bamboo rings are bonded to the face skins using a polyurethane structural adhesive. The product is referred to as "Bamboo Core Sandwich" (BCS) panel and is shown in Figure 1(b). Bamboo is a sustainable natural material and can be recycled. Bamboo is fast-growing (harvested in 3–4 years from the time of planting) and has mechanical properties comparable to those of conventional building materials [17].

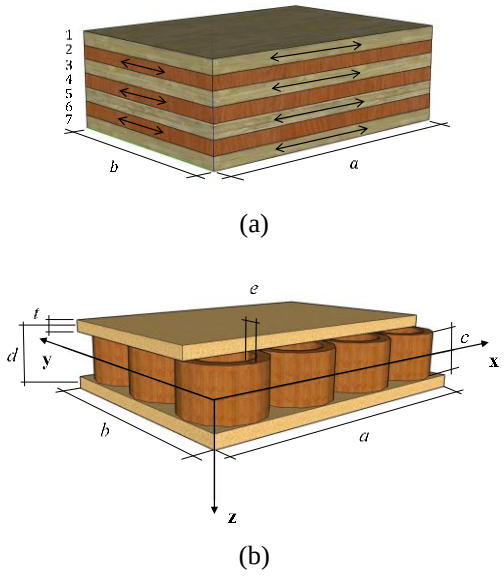

Figure 1: *A schematic illustration of the (a) existing commercial Cross-Laminated Timber (CLT) panel, and (b) proposed composite Bamboo Core Sandwich (BCS) panel*

In this paper, the flexural behaviour of the proposed BCS panel under a uniform transverse pressure is studied using the Ritz-method (energy method). Effects of the thickness of the plywood skins and height of the bamboo core on the bending stiffness of the BCS panels are presented. The results are compared to the bending stiffness of commercially available CLT panels of almost similar depths.

2 METHODOLOGY AND VALIDATION

The flexural behaviour of the BCS panel under a uniform transverse pressure, with two-edge simply supported (one-way bending) and four-edge simply supported (two-way bending) configurations is investigated using the Ritz-method. In this method, the total energy of the system, which consists of the potential energy of the core, membrane and local bending strain energies of the faces, is calculated. Due to difference in stiffness of the core compared to the plywood faces, the energy terms incorporate the shearing strain of the core in orthogonal directions and purely in-plane shearing strain of the faces. It is worth noting that the core behaviour may not follow the same assumption as has been adopted by many researchers for common types of core materials such as foam. The in-plane stiffness (*xy* plane in Figure 1(b)) of common core materials are much less stiff than the faces; therefore, their contribution to the flexural rigidity of the sandwich panel is neglected. In the Ritz-method, by assuming an appropriate expression for the deflection of the orthotropic plate and considering the boundary conditions of BCS panel, the total energy of the system is minimised and the maximum deflection is calculated. Various stages of the problem formulation and corresponding equations are discussed below to determine the maximum mid-span displacement of the panel under a uniform distributed load.

2.1 THE RITZ METHOD

An elevation of a short length *dx* of the sandwich panel (*xz* plane) with thin identical faces is shown in Figure 2. The figure demonstrates the deformed and undeformed cross-sections of the sandwich panel. During the subsequent displacement, if there were no shear strains, the line *abcde*, which is normal to the centre line of the undeformed panel, would rotate through an angle *dw/dx* to the position *a'b'c'd'e'* and remain normal to the centre line of the sandwich panel. Since the BCS panel does not have an antiplane or flexible core (contributes to flexural rigidity of the sandwich), the line *abcde* moves to a new position *a"b"c'd"e"* during the subsequent displacement, where *d'c'd"=γ*. However, the lines *a"b"* and *d"e"* remain parallel with *a'b'c'd'e'* as the shear strains in the faces are assumed negligible. The model makes allowance for the effect of face thickness on the geometry of the deformation and for the local bending stiffness of the faces. The angle *d"c'z* is denoted as λ (*dw/dx*), where λ is a coefficient that may take any values between one (core rigid in shear) and zero (completely flexible core).

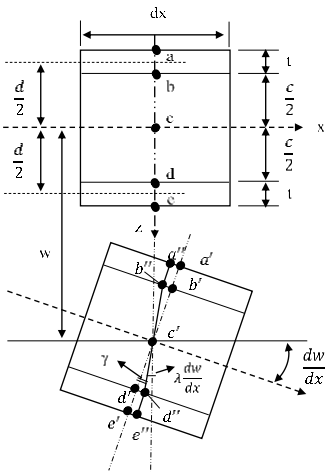

Figure 2: *A short length (dx) of a sandwich panel with a stiff core, before and after deformation*

A similar diagram may be drawn for the *yz* plane to obtain the displacement in *y* direction. In this case, μ would be a parameter such that a line in the core, which is originally vertical, rotates in the *yz* plane through an

angle μ (dw/dy). Then the displacements (u) and (v) in x and y directions of various points are determined based on the distorted cross-section (Figure 2) as follows:

(a) Displacement field in the core:

$$u_c = -z\lambda\frac{\partial w}{\partial x}, \quad -\frac{c}{2} \le z \le +\frac{c}{2} \tag{1a}$$

$$v_c = -z\mu\frac{\partial w}{\partial y}, \quad -\frac{c}{2} \le z \le +\frac{c}{2} \tag{2b}$$

(b) Displacement field in the lower face:

$$\begin{aligned} u_f &= -\frac{c}{2}\lambda\frac{\partial w}{\partial x} - \left(z - \frac{c}{2}\right)\frac{\partial w}{\partial x} \\ &= -\left\{\frac{c}{2}(\lambda - 1) + z\right\}\frac{\partial w}{\partial x}, \quad \frac{c}{2} \le z \le \frac{h}{2} \end{aligned} \tag{2a}$$

$$v_f = -\left\{\frac{c}{2}(\mu - 1) + z\right\}\frac{\partial w}{\partial y}, \quad \frac{c}{2} \le z \le \frac{h}{2} \tag{2b}$$

(c) Displacement field in the mid-plane of the lower face:

$$u_{fm} = -\frac{1}{2}(c\lambda + t)\frac{\partial w}{\partial x}, \quad z = \frac{c+t}{2} \tag{3a}$$

$$v_{fm} = -\frac{1}{2}(c\mu + t)\frac{\partial w}{\partial y}, \quad z = \frac{c+t}{2} \tag{3b}$$

where c is the core height, t is the face thickness and h is the overall depth of the panel as shown in Figure 2.

The expressions for the strains are obtained by differentiation of the above displacements u and v within the corresponding displacement fields, and in x and y directions, respectively.

The strains in the core are:

$$\in_x^c = \frac{\partial u}{\partial x} = -z\lambda\frac{\partial^2 w}{\partial x^2} \tag{4a}$$

$$\in_y^c = \frac{\partial v}{\partial y} = -z\mu\frac{\partial^2 w}{\partial y^2} \tag{4b}$$

$$\gamma_{zx}^c = \frac{\partial u}{\partial z} + \frac{\partial w}{\partial x} = (1 - \lambda)\frac{\partial w}{\partial x} \tag{4c}$$

$$\gamma_{yz}^c = \frac{\partial v}{\partial z} + \frac{\partial w}{\partial y} = (1 - \mu)\frac{\partial w}{\partial y} \tag{4d}$$

$$\gamma_{xy}^c = \frac{\partial u}{\partial y} + \frac{\partial v}{\partial x} = -z(\lambda + \mu)\frac{\partial^2 w}{\partial x \partial y} \tag{4e}$$

The strains in the faces consist of membrane and local bending strains. Membrane strains at the middle plane of the faces are obtained by differentiation of Eqs. 3a and 3b:

$$\in_x^{fm} = \frac{\partial u}{\partial x} = -\frac{1}{2}(c\lambda + t)\frac{\partial^2 w}{\partial x^2} \tag{5a}$$

$$\in_y^{fm} = \frac{\partial v}{\partial y} = -\frac{1}{2}(c\mu + t)\frac{\partial^2 w}{\partial y^2} \tag{5b}$$

$$\gamma_{xy}^{fm} = \frac{\partial u}{\partial y} + \frac{\partial v}{\partial x} = -\frac{\partial^2 w}{\partial x \partial y}\left(\frac{c}{2}\lambda + \frac{c}{2}\mu + t\right) \tag{5c}$$

Local bending strains (Eqs. 6c-6e) are the strains at the mid-planes of the faces, obtained by differentiation of the displacement field within the faces (Eqs. 6a and 6b).

$$u_{fL} = -\left\{\frac{c}{2}(\lambda - 1) + z\right\}\frac{\partial w}{\partial x} + \frac{1}{2}(c\lambda + t)\frac{\partial w}{\partial x} = -\left(z - \frac{c}{2} - \frac{t}{2}\right)\frac{\partial w}{\partial x} \tag{6a}$$

$$v_{fL} = -\left\{\frac{c}{2}(\mu - 1) + z\right\}\frac{\partial w}{\partial y} + \frac{1}{2}(c\mu + t)\frac{\partial w}{\partial y} = -\left(z - \frac{c}{2} - \frac{t}{2}\right)\frac{\partial w}{\partial y} \tag{6b}$$

$$\in_x^{fL} = -\left(z - \frac{c}{2} - \frac{t}{2}\right)\frac{\partial^2 w}{\partial x^2}, \quad \frac{c}{2} \le z \le \frac{h}{2} \tag{6c}$$

$$\in_y^{fL} = -\left(z - \frac{c}{2} - \frac{t}{2}\right)\frac{\partial^2 w}{\partial y^2}, \quad \frac{c}{2} \le z \le \frac{h}{2} \tag{6d}$$

$$\gamma_{xy}^{fL} = \frac{\partial u}{\partial y} + \frac{\partial v}{\partial x} = -2\left(z - \frac{c}{2} - \frac{t}{2}\right)\frac{\partial^2 w}{\partial x \partial y} \tag{6e}$$

The total direct strain in the lower face is calculated through the summation of membrane and local bending strains. For instance, the total direct strain in the lower face is the sum of the Eqs. 5a and 6c in x direction or the sum of the Eqs. 5b and 6d in the y direction. Once the strains expressions are obtained, the strain energy U per unit volume of the orthotropic elastic solid is calculated.

$$\begin{aligned} U &= \frac{1}{2g}\int_V \left\{E_x \in_x^2 + E_y \in_y^2 + 2E_x \nu_{yx} \in_x \in_y\right\} dV \\ &+ \frac{1}{2}\int_V \left\{G_{zx}\gamma_{zx}^2 + G_{xy}\gamma_{xy}^2 + G_{yz}\gamma_{yz}^2\right\} dV \end{aligned} \tag{7}$$

where E_x, E_y, G_{xy}, G_{yz}, G_{xz} are the various elastic and shear moduli, υ_x, υ_y are the Poisson's ratios and g is equal to $(1-\upsilon_x\upsilon_y)$.

The strain energy in the core (Eq. 8), is obtained by substitution of Eqs. 4a-4e into Eq. 7. Unlike previous studies with flexible core materials which neglect the core stiffness, the strain energy in the proposed bamboo core, includes the in-plane stiffness of the core. The shear stiffness in the xy plane of the core is also considered in the present model. The strain energy due to direct stresses and strains in the z direction is neglected due to high stiffness of the core materials in z direction (low possibility of significant flattening or squashing) and small intensity of transverse load.

$$U_c = \frac{1}{2g}\int_V \begin{Bmatrix} E_x\left(-z\lambda\frac{\partial^2 w}{\partial x^2}\right)^2 + E_y\left(-z\mu\frac{\partial^2 w}{\partial y^2}\right)^2 \\ +2E_x\nu_{yx}\left(-z\lambda\frac{\partial^2 w}{\partial x^2}\right)\left(-z\mu\frac{\partial^2 w}{\partial y^2}\right) \end{Bmatrix} dV + \frac{1}{2}\int_V \begin{Bmatrix} G_{zx}\left((1-\lambda)\frac{\partial w}{\partial x}\right)^2 + G_{xy}\left(-z(\lambda+\mu)\frac{\partial^2 x}{\partial x\partial y}\right)^2 \\ +G_{yz}\left((1-\mu)\frac{\partial w}{\partial y}\right)^2 \end{Bmatrix} dV \quad (8)$$

To determine the strain energy in the core, the integration is carried out over the volume of the core and the area of the panel respectively. Since the bamboo core does not have the same area as the faces (dissimilar to regular core materials such as foam), the following factor (K_{Bamboo}) has been introduced to consider the contribution of core area in the derivation of the strain energy of the core. To do this, the modulus of elasticity (MOE) and shear modulus (G) of the bamboo core are multiplied by the modification factor in Eq. 9. The factor equals the ratio of the present volume of the core material (bamboo) over the total available core volume space in the panel.

$$K_{Bamboo} = \left[\frac{\pi\left(R^2 - r^2\right)\times c}{abc}\right]\times n \quad (9)$$

where R, r and c are the outer radius, inner radius and the height of the bamboo hollow sections, respectively. The total number of bamboo rings within the panel is shown with n.

The strain energy of the lower face is calculated by Eq. 10, after substituting Eqs. 5a-5c into Eq. 7 and integrated over the thickness of the plywood face and area of the panel. An identical expression is obtained for the upper face sheet of plywood.

$$U_{fm} = \frac{1}{2}\int_V \begin{Bmatrix} \frac{E_x\left(-\frac{1}{2}(c\lambda+t)\frac{\partial^2 w}{\partial x^2}\right)^2}{g} + \frac{E_y\left(-\frac{1}{2}(c\mu+t)\frac{\partial^2 w}{\partial y^2}\right)^2}{g} \\ +\frac{2E_x\nu_{yx}\left(-\frac{1}{2}(c\lambda+t)\frac{\partial^2 w}{\partial x^2}\right)\left(-\frac{1}{2}(c\mu+t)\frac{\partial^2 w}{\partial y^2}\right)}{g} \\ +G_{xy}\left(-\frac{\partial^2 w}{\partial x\partial y}\left(\frac{c}{2}\lambda+\frac{c}{2}\mu+t\right)\right)^2 \end{Bmatrix} dV \quad (10)$$

The stress in z direction is assumed negligible, as the intensity of a transverse distributed load is much smaller than the magnitude of the stresses in the parallel direction. The shear strain energy in zx and yz planes are also neglected because the plywood faces are shallow in proportion to their spans.

The strain energy due to bending in the lower face is calculated by substituting Eqs. 6c-6e into Eq. 7 and integrating over the thickness of the plywood skin and the area of the panel. The strain energy due to bending in the upper face is calculated similarly.

$$U_{fb} = \frac{1}{2}\int_V \begin{Bmatrix} \frac{E_x\left(-\left(z-\frac{c}{2}-\frac{t}{2}\right)\frac{\partial^2 w}{\partial x^2}\right)^2}{g} + \frac{E_y\left(-\left(z-\frac{c}{2}-\frac{t}{2}\right)\frac{\partial^2 w}{\partial y^2}\right)}{g} \\ +\frac{2E_x\nu_{yx}\left(-\left(z-\frac{c}{2}-\frac{t}{2}\right)\frac{\partial^2 w}{\partial x^2}\right)\left(-\left(z-\frac{c}{2}-\frac{t}{2}\right)\frac{\partial^2 w}{\partial y^2}\right)}{g} \\ +G_{xy}\left(-2\left(z-\frac{c}{2}-\frac{t}{2}\right)\frac{\partial^2 w}{\partial x\partial y}\right)^2 \end{Bmatrix} dV \quad (11)$$

The change of potential energy associated with the deformation of the orthotropic sandwich plate under the applied uniformly distributed load q is:

$$V = -\int_0^a\int_0^b wqdxdy = -q\int_A wdA \quad (12)$$

The uniformly distributed load q can be represented by a double Fourier series expansion.

$$q_{uni} = \sum_{m=1}^{\infty}\sum_{n=1}^{\infty}\frac{16q}{\pi^2 mn}\sin\left(\frac{m\pi x}{a}\right)\sin\left(\frac{n\pi y}{b}\right) \quad (13)$$

where a and b are the length and width of the panel. Similarly, for a point load (local pressure applied over a small rectangular area with length a' and width b' and centre located at (ξ,η)) can be shown in following Fourier format:

$$q_{point} = \sum_{m=1}^{\infty}\sum_{n=1}^{\infty}\frac{16P}{\pi^2 mna'b'}\sin\left(\frac{m\pi\xi}{a}\right)\sin\left(\frac{n\pi\eta}{b}\right) \times\sin\left(\frac{m\pi a'}{2a}\right)\sin\left(\frac{n\pi b'}{2b}\right)\sin\left(\frac{m\pi x}{a}\right)\sin\left(\frac{n\pi y}{b}\right) \quad (14)$$

Since the deflection and bending moments at the simply supported edges are zero,

$$w = 0,\quad \frac{\partial^2 w}{\partial x^2} = 0 \quad \text{for} \quad x = 0 \ \text{and} \ x = a$$

$$w = 0,\quad \frac{\partial^2 w}{\partial y^2} = 0 \quad \text{for} \quad y = 0 \ \text{and} \ y = b$$

the displacement field w for the four-edge and the two-edge simply supported plates which satisfy the boundary conditions above, are defined by Eqs. 15a and 15b, respectively.

$$w = \sum_{m=1}^{\infty}\sum_{n=1}^{\infty}a_{mn}\sin\left(\frac{m\pi x}{a}\right)\sin\left(\frac{n\pi y}{b}\right) \quad (15a)$$

$$w = \sum_{m=1}^{\infty}a_m\sin\left(\frac{m\pi x}{a}\right) \quad (15b)$$

The total energy of system ($\Pi = U + V$) is the summation of Eqs. 8, 10, 11 and 12. Eqs. 10 and 11 are counted twice to account for the upper and lower faces. Π is a function of a_{mn}, λ and μ. These parameters are calculated by minimising the total energy using the following system of equations.

$$\frac{\delta}{\delta\lambda}(U+V)=\frac{\delta}{\delta\mu}(U+V)=\frac{\delta}{\delta a_{mn}}(U+V)=0 \quad (16)$$

2.2 VALIDATION OF THE RITZ METHOD

The Ritz-method is validated by comparing the load-deflection response of a square 600×600 mm Glass Fibre Reinforced Polymer (GFRP) sandwich panel, from the proposed Ritz-method and experimental results reported in [18]. The sandwich panel used in the study is made of glass fibre composite skins with wall thickness of 3 mm and a modified phenolic core with depth of 12 mm, co-cured using a toughened phenol formaldehyde resin. The GFRP skin had a modulus of elasticity 11750 MPa and a shear modulus of 2465 MPa, while the modified core had a modulus of elasticity 1350 MPa with a shear modulus of 746 MPa. The slab was supported on four sides while loaded at mid-point. Steel screws were used to fix the GFRP sandwich slab to the timber support to represent the simply supported conditions. The point load was applied via a 100×100 mm steel plate at the centre of the plate. The predicted and measured load-deflection responses of the GFRP slab are compared in Figure 3. The measured deflections were taken at the centre of the panel under the point load. As shown in Figure 3, reasonable correlation is observed between the Ritz-method and the experimental results within the linear region. The maximum difference between stiffness found from the experimental test and the Ritz-method is less than 4%.

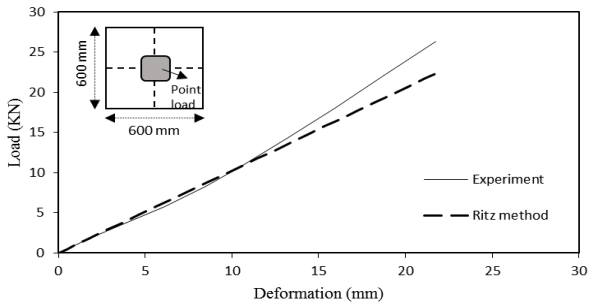

Figure 3: *Comparison of numerical and experimental response of the GFRP sandwich panel*

3 PARAMETRIC DEPENDENCY OF FLEXURAL STIFFNESS OF BCS PANELS

A parametric study is conducted using the validated Ritz-method to evaluate the effect of various parameters on flexural stiffness of the BCS panels. The influence of the skin thickness, core height and support conditions (two-edge and four-edge simply supported) are investigated. In addition, the maximum deflection of the BCS panels are benchmarked against those of CLT panels with almost identical depths. Deflections of the CLT panels are calculated using the Shear Analogy Method, which is an accepted method used by industry and includes the effect of shear deformation [19]. In this method, the maximum theoretical deflection value Δ_{CLT} in the middle of the CLT panel under a uniform distributed load is obtained as sum of the flexural and shear deflections.

3.1 MATERIAL PROPERTIES

Three different standard types of commercial plywood according to Australian/New Zealand standard [20], manufactured from a single species, plantation pine (*Pinus Radiata*) are adopted for the skins. The material properties of *Radiata* are shown in Table 1. The *x* axis is parallel to the grain and the *y* axis is perpendicular to the grain. In the study that follows, each structural plywood sheet is labelled by a standard identification code, which provides the nominal plywood thickness, the face veneer thickness multiplied by 10 and the number of the constituent plies in the assembly. For instance, the ID code (18-30-7) in Table 2, describes an 18 mm thick plywood of 3 mm face veneer thickness with 7 veneer layers. To find the mechanical properties of the plywood skins from orthotropic properties of each veneer (*Radiata* plies), OSULaminates is utilised, which is a Java Application developed by Oregon State University for analysis of laminated plates [21]. OSULaminates uses classical laminate theory to calculate the axial and bending rigidity of laminated plates based on the input layer properties. The material properties of the plywood sheets obtained by OSULaminate are shown in Table 3. The properties of the bamboo are taken as the average values of *Moso* bamboo (*Phyllostachys pubescens)* reported in [22] (Table 3).

For sake of comparison, two commercial CLT panels, *CL7/295* and *CL7/315* have been selected from XLam structural design tables [23]. The panels consist of seven layers of sawn boards with a total thickness of 295 mm and 315 mm, respectively. The two outermost layers, 1 and 7 and of the middle layers, 3 and 5 are extended in the direction of the length of the element whereas the other layers are perpendicular to span direction. As shown in Table 4, the modulus of elasticity of the outer longitudinal layers are higher than the internal laminates, because the CLT panels gain the majority of their stiffness from the outer laminates. The internal laminates hold the structural layers apart and do not require higher structural properties. The material properties of the CLT panels in this study have been taken from XLam design guide.

3.2 NARROW PANELS

To evaluate the one-way flexural behaviour of the BCS panel under a uniform distributed load (5 kPa), three sandwich panels with varied aspect ratios were selected. Sandwich panels of 4, 6 and 7 m spans but with similar width of 1 m are modelled using the developed Ritz-method. Figure 4(a) shows the maximum deflection of the 4 m BCS panels (two-edge simply supported) with three plywood IDs. The basic panel configuration considered include skin thickness of 18 mm with an overall panel depth of 122 mm. Total depth of the panel is then increased by rising the core height (*c*) and thickness of the commercial plywood skins (*t*). However, in all cases the ratio of the centroid of the faces to the face thickness (*d/t*) is kept between 5.77 and 100 to comply with the requirements of thin face sandwich panels [24]. The maximum deflection of the CLT panel (*CL7/295*) with a total depth of 295 mm is also plotted to provide a benchmark against the BCS panels. By

increasing the depth of the panel (*c* and *t*), the mid-span deflection (*Δ*) drops drastically. The minimum deflection occurs in BCS (21-30-9) with a total panel depth of 284 mm. According to the material properties in Table 2, this optimum result in BCS (21-30-9) is associated with the higher MOE of its plywood skins in longitudinal direction. Similar trends are observed in the 6 and 7 m BCS panels of different plywood skins in Figures 4(b) and 4(c). The most favourable results correspond to BCS (21-30-9) in comparison with CLT panels of almost similar depths.

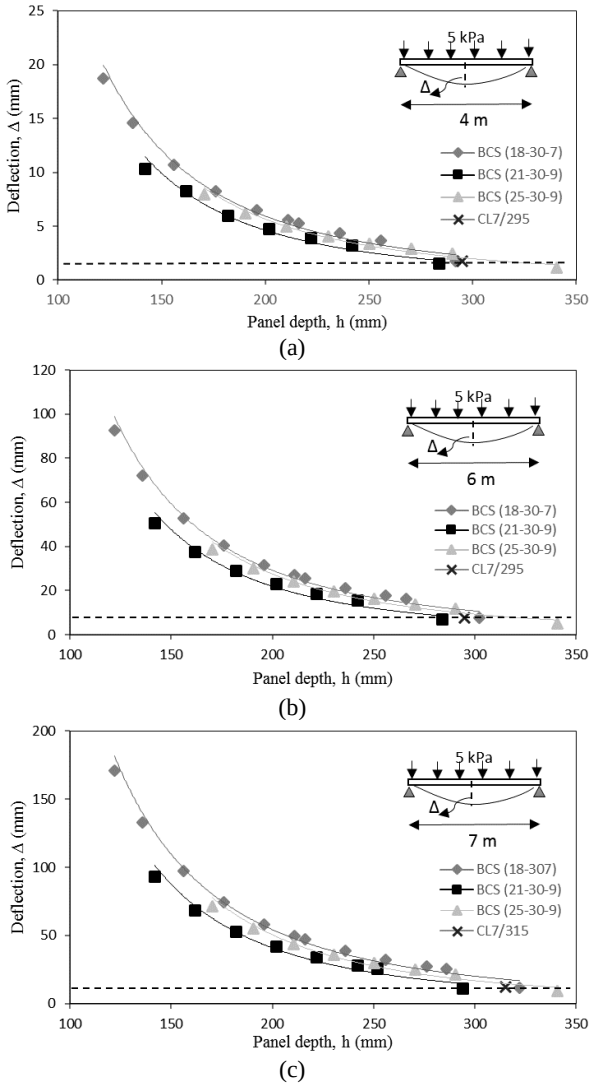

Figure 4: *Maximum deflection of BCS and CLT panels in one-way bending considering (a) 4 m span (b) 6 m span and (c) 7 m span*

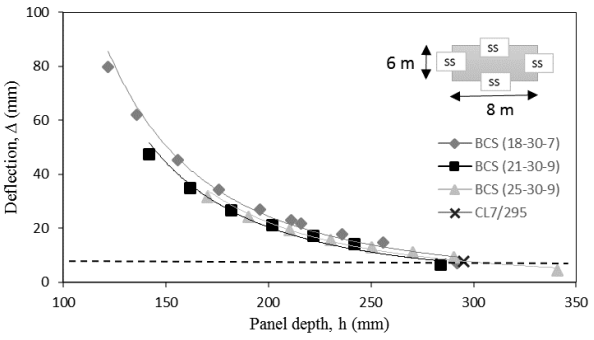

Figure 5: *Maximum deflection of BCS and CLT panels in two-way bending*

3.3 WIDE PANELS

Two-way flexural behaviour of the proposed sandwich panels under a uniform distributed load is investigated, by modelling 6×8 m panels with three different plywood skin configurations, similar to narrows panels. The maximum deflections of BCS and CLT panels (6×8 m) in two-way bending in correspondence with total depth of the panels are shown in Figure 5. Similar to one-way bending response, the BCS panel with plywood skin ID (21-30-9) yields the optimum results, with a depth almost 4% smaller than *CL7/295* panel.

4 COMPARISON BETWEEN FLEXURAL STIFFNESS OF THE BCS AND CLT PANELS

Table 5 shows the flexural properties of the BCS panels, commercial CLT panels and their corresponding deflections and weight ratios. The deflections of the CLT panels are calculated based on the shear analogy method and are compared with the deflections of selected BCS panels obtained from the Ritz-method. The selected BCS panels are the panels with the optimum results among the three types of plywood skins in each span, as demonstrated in Figures 4(a)-4(c) for one-way bending, and Figure 5, for two-way bending configurations. Using the 6 m span BCS (21-30-9) panel with a total depth of 284 mm, nearly 12% reduction in transverse deflection can be achieved in comparison with *CL7/295*. The aforementioned CLT panel is a 7-layer CLT panel with a total depth of 295 mm. The BCS (21-30-9) panel is also almost 14% lighter with a total weight of less than 92 kg/m^2. Likewise, the one-way bending behaviour of the 4 and 7 m BCS (21-30-9) panels depict higher bending stiffness than CLT panels, with a minimum of 40% reduction in weight per square meter. The stiffness and weight ratios of the 6×8 m, four-edge simply supported BCS and CLT panels are also presented in Table 5. Comparing the efficiencies of the panels in two-way bending, it can be concluded that the BCS panel shows 15% higher bending stiffness than the CLT panel, with nearly 40% reduction in weight.

5 CONCLUSIONS

An innovative sandwich composite panel, the “Bamboo Core Sandwich” (BCS) panel, was proposed for flooring system in buildings. The flexural behaviour of the panel was investigated numerically, using a proposed energy method (the Ritz-method) which accounts for the in-plane and shear stiffness of the core. The method was validated against published results of an experimental test on GFRP sandwich panels. The effects of the thickness of the plywood skins and height of the bamboo core on the flexural stiffness of BCS panels were studied under one-way and two-way bending actions. Results showed that the mechanical properties of the plywood skins, contribute significantly to the flexural stiffness of BCS panels. In either one-way action (narrow panels) or two-way action (wide panels), the optimum results were observed in the BCS (21-30-9) panel. This panel has the higher MOE of the plywood skins in span direction, amongst other BCS panels. Results of the optimum BCS configuration in narrow and wide panels were then compared to commercial CLT panels of almost identical

depths, to evaluate the efficiency of the proposed BCS panel in terms of stiffness and total weight. It was understood that, in one-way bending, using BCS (21-30-9) narrow panel with a total depth of 284 mm and length of 6 m, the deflection and total weight were reduced by 12% and 40% respectively, when compared to the *CL7/295*. In two-way bending, the BCS (21-30-9) wide panel with depth of 284 mm and length of 6 m showed to be 15% stiffer and 40% lighter than the commercial CLT panel.

Table 1: *Material properties of Radiata*

Species	Modulus of elasticity	Poison's ratio	Shear modulus
Radiata	E_X=15,070 MPa	υ_{XY}=0.444 MPa	G_{XY}=798 MPa
	E_Y=678 MPa	υ_{YX}=0.387 MPa	G_{YZ}=150 MPa
	E_Z=1,115 MPa	υ_{XZ}=0.392 MPa	G_{XZ}=829 MPa

Table 2: *Material properties of plywood skins in Ritz method*

Material	Plywood ID	MOE Longitudinal (MPa)	MOE Transverse (MPa)	Shear Modulus (MPa)	Poisson's ratio (*yx*-plane)
Plywood	(18-30-7)	9,382	6,483	799	0.03
Plywood	(21-30-9)	11,037	4,824	799	0.02
Plywood	(25-30-9)	8,278	7,587	799	0.03

Table 3: *Material properties of bamboo core in Ritz method*

Material	MOE Longitudinal (MPa)	MOE Radial (MPa)	MOE Circumferential (MPa)	Shear Modulus (MPa)	Poisson's ratio
Bamboo	10,500	1,260	1,260	630	0.3

Table 4: *Material properties of the boards in CLT panels*

Material	MOE Longitudinal (MPa)	MOE Transverse (MPa)	Shear Modulus (parallel to span) (MPa)	Shear Modulus (perpendicular to span) (MPa)
External laminations	8,000	360	440	80
Internal laminations	6,000	270	330	60

Table 5: *Properties of BCS (21-30-9) and CLT panels and corresponding deflections and weight ratios*

		CLT			BCS						Results	
a (m)	b (m)	h (mm)	Δ (mm)	w (kg/m^2)	h (mm)	c (mm)	t (mm)	Δ (mm)	w_{bamboo}/ $w_{plywood}$	w_{total} (kg/m^2)	$w_{(BCS)}$/ $w_{(CLT)}$	$k_{(BCS)}$/ $k_{(CLT)}$
4	1	295	1.75	150	284	200	42	1.49	0.84	91.38	0.61	1.17
6	1	295	7.64	150	284	200	42	6.75	0.84	91.38	0.61	1.13
7	1	315	12	161	294	210	42	11.2	0.89	93.48	0.58	1.06
6	8	295	7.29	150	284	200	42	6.36	0.84	91.38	0.61	1.15

REFERENCES

[1] Manalo, A., Aravinthan, T., Karunasena, W., & Ticoalu, A. A review of alternative materials for replacing existing timber sleepers. *Composite structures*, *92*(3), 603-611, 2010.

[2] Liew, J. R., & Sohel, K. Structural performance of steel-concrete-steel sandwich composite structures. *Advances in Structural Engineering*, *13*(3), 453-470, 2010.

[3] Dawood, M., Taylor, E., & Rizkalla, S. Two-way bending behavior of 3-D GFRP sandwich panels with through-thickness fiber insertions. *Composite structures*, *92*(4), 950-963, 2010.

[4] Sohel, K., & Liew, J. R. Steel–Concrete–Steel sandwich slabs with lightweight core—Static performance. *Engineering structures*, *33*(3), 981-992, 2011.

[5] Grenestedt, J. L., & Bekisli, B. Analyses and preliminary tests of a balsa sandwich core with improved shear properties. *International journal of mechanical sciences*, *45*(8), 1327-1346, 2003.

[6] Mamalis, A., Spentzas, K., Manolakos, D., Ioannidis, M., & Papapostolou, D. Experimental investigation of the collapse modes and the main crushing characteristics of composite sandwich panels subjected to flexural loading. *International journal of crashworthiness*, *13*(4), 349-362, 2008.

[7] Reis EM, Rizkalla SH. Material characteristics of 3-D FRP sandwich panels. Constr Build Mater 2008;22(6):1009–18.

[8] Reyes, G. Static and low velocity impact behavior of composite sandwich panels with an aluminum foam core. *Journal of Composite Materials*, *42*(16), 1659-1670, 2008.

[9] McCormack, T., Miller, R., Kesler, O., & Gibson, L. Failure of sandwich beams with metallic foam cores. *International Journal of Solids and Structures*, *38*(28), 4901-4920, 2001.

[10] Nia, A. A., & Sadeghi, M. The effects of foam filling on compressive response of hexagonal cell aluminum honeycombs under axial loading-experimental study. *Materials & Design*, *31*(3), 1216-1230, 2010.

[11] Gagnon, S., & Pirvu, C. CLT Handbook-Canadian Edition Chapter 3: Structural design of corss laminated timber elements. In: FPInnovations, 2011.

[12] Sharaf, T., Shawkat, W., & Fam, A. Structural performance of sandwich wall panels with different foam core densities in one-way bending. *Journal of Composite Materials*, *44*(19), 2249-2263, 2010.

[13] Styles, M., Compston, P., & Kalyanasundaram, S. The effect of core thickness on the flexural behaviour of aluminium foam sandwich structures. *Composite structures*, *80*(4), 532-538, 2007.

[14] Daniel, I. M., & Abot, J. L. Fabrication, testing and analysis of composite sandwich beams. *Composites Science and Technology*, *60*(12), 2455-2463, 2000.

[15] Dai, J., & Hahn, H. T. Flexural behavior of sandwich beams fabricated by vacuum-assisted resin transfer molding. *Composite structures*, *61*(3), 247-253, 2003.

[16] Mahfuz, H., Islam, M. S., Rangari, V. K., Saha, M. C., & Jeelani, S. Response of sandwich composites with nanophased cores under flexural loading. *Composites Part B: Engineering*, *35*(6), 543-550, 2004.

[17] Van der Lugt, P., Van den Dobbelsteen, A., & Janssen, J. An environmental, economic and practical assessment of bamboo as a building material for supporting structures. *Construction and building materials*, *20*(9), 648-656, 2006.

[18] Awad, Z. K., Aravinthan, T., Zhuge, Y., & Manalo, A. Geometry and restraint effects on the bending behaviour of the glass fibre reinforced polymer sandwich slabs under point load. *Materials & Design*, *45*, 125-134, 2013.

[19] Gagnon, S., & Pirvu, C. CLT Handbook-Canadian Edition: FPInnovations, 2011.

[20] Australian/New Zealand Standard. AS/NZS 2269.0:2012 Plywood-Structural Part 0: Specification, 2012.

[21] John A. Nairn. OSULaminates (Version version 6.0): Oregon state university, 2015.

[22] Chung, K., & Yu, W. Mechanical properties of structural bamboo for bamboo scaffoldings. *Engineering structures*, *24*(4), 429-442, 2002.

[23] XLam. (2016). Designing with XLam Cross Laminated Timber. New Zealand Edition.

[24] Allen, H. G. Analysis and design of structural sandwich panels: Pergamon Press, oxford, 1969.